Published in final edited form as:

J Immunol. 2018 September 15; 201(6): 1705–1716. doi:10.4049/jimmunol.1800202.

The Phagocyte Oxidase Controls Tolerance to *Mycobacterium tuberculosis* infection.

Andrew J Olive[1], **Clare M Smith**[1], **Michael C Kiritsy**[1], and **Christopher M Sassetti**[1,2]

[1]University of Massachusetts Medical School, Worcester MA

[2]Corresponding Author

Summary

Protection from infectious disease relies on two distinct strategies: antimicrobial "resistance" directly inhibits pathogen growth, whereas infection "tolerance" protects from the negative impact of infection on host health. A single immune-mediator can differentially contribute to these strategies in distinct contexts, confounding our understanding of protection to different pathogens. For example, the NADPH-dependent phagocyte oxidase complex (Phox) produces antimicrobial superoxide and protects from tuberculosis (TB) in humans. However, Phox-deficient mice display no sustained resistance defects to *M. tuberculosis*, suggesting a more complicated role for NADPH phagocyte oxidase complex than strictly controlling bacterial growth. We examined the mechanisms by which Phox contributes to protection from TB and found that mice lacking the Cybb subunit of Phox suffered from a specific defect in tolerance, which was due to unregulated Caspase 1 activation, interleukin 1β (IL-1β) production, and neutrophil influx into the lung. These studies imply that a defect in tolerance alone is sufficient to compromise immunity to *Mtb* and highlight a central role for Phox and Caspase 1 in regulating TB disease progression.

Introduction

Protective defense to infectious disease involves functionally overlapping responses that can be divided into two fundamentally different categories (1, 2). Infection "resistance" refers to functions that directly target the infecting pathogen to prevent its growth and dissemination. Resistance pathways act by a variety mechanisms including disrupting the bacterial niche, serving as metabolic poisons, and sequestering critical nutrients (3–5). In addition, the extent of disease is also influenced by "tolerance" strategies that enhance host survival but do not directly impact pathogen growth (6–8). Tolerance pathways control a broad range of functions that protect the infected tissues from the direct cytotoxic properties of the pathogen, the inflammation-mediated immunopathology, and enhance the overall health of the host in the face of an ongoing infection. While it is well appreciated that both resistance and tolerance mechanisms are required to limit disease, the relative importance of these pathways vary for different infections (1). Furthermore, since individual immune effectors

Author Contributions

AO and CMSassetti conceived of and designed the experiments. AO, CMSmith, and MK performed the experiments and analyzed the data. AO and CMSasssetti wrote the initial manuscript. All authors edited the manuscript.

can promote both tolerance and resistance, the specific role for each mediator can change in different contexts (1, 6, 9–11). In the context of chronic infections, where resistance mechanisms are insufficient and the pathogen persists in the tissue, tolerance is likely to play a particularly important role (11).

Like many other chronic infections, the outcome of an encounter with *Mycobacterium tuberculosis* (*Mtb*) varies dramatically between individuals (12). Only 5–10% of those that are infected with this pathogen progress to active tuberculosis (TB), and disease progression is influenced by a wide-variety of genetic and environmental factors that modulate either tolerance or resistance (13–15). For example, observations from humans and mice indicate that several specific changes in T cell function may contribute to a failure of resistance and disease progression due to loss of antimicrobial resistance (16–18). In addition, studies in animal models indicate that a failure of host tolerance, which is necessary to preserve lung function or granuloma structure, influences the extent of disease (19, 20). While these studies suggest that variation in overall tolerance may be an important determinant TB risk, the specific tolerance mechanisms that influence disease progression in natural populations remain ill defined. Furthermore, since most immune mediators are pleiotropic and affect both tolerance and resistance, it remains unclear if a specific failure of tolerance alone can promote TB disease progression.

During many bacterial infections the production of reactive oxygen species (ROS) by the NADPH phagocyte oxidase (Phox) is involved in protecting the host from disease (21). Phox is a multi-protein complex, including the subunits Cybb (gp91) and Ncf1 (p47) that assemble in activated immune cells to produce superoxide radicals by transferring electrons from NADPH to molecular oxygen (22). Humans with deleterious mutations in the Phox complex develop a clinical syndrome known as chronic granulomatous disease (CGD). Leukocytes from patients with CGD are unable to kill a number of bacterial pathogens, such as *Staphylococcus aureus* and *Serratia marcescens,* and this defect is associated with the susceptibility to infection with these organisms (23). Because ROS contributes to the microbicidal activity of phagocytes, previous studies in *Mtb*-infected mice focused on the role of Phox in antimicrobial resistance. Several such studies found that mice deficient in Phox show no long-term differences in *Mtb* bacterial levels compared to wild type animals (24–26) . Cooper et al observed a transient increase in bacterial numbers between 15 and 30 days after infection of $Ncf1^{-/-}$ mice, but this difference was not sustained (24). Two subsequent studies found that no difference in Mtb burden could be attributed to Cybb deficiency (25, 26). The lack of an obvious antimicrobial role for Phox during *Mtb* infection is likely due to the expression of mycobacterial ROS defenses. These defenses include the catalase/peroxidase, KatG, which detoxifies ROS directly, and the MRC complex that detoxifies a variety of radicals (26–29). Together these bacterial defense mechanisms may allow *Mtb* to withstand the oxidative killing mechanisms (30). In contrast to the apparent dispensability of Phox in short-term mouse infections with *Mtb*, human mutations in the *Cybb* gene are strongly associated with susceptibility to mycobacterial diseases, including TB (31–35). Mutations that specifically reduce Cybb activity in macrophages produce a similar clinical presentation, highlighting the importance of the macrophage-derived ROS in protection (31). Taken together, while Phox is clearly important for controlling mycobacterial diseases including TB, the absence of long-term resistance defects in *Mtb*-

infected mice suggest that the phagocyte oxidase may play a more complex role than simply limiting bacterial replication.

Here we examined the mechanisms of Phox-mediated protection in the context of *Mtb* infection. We found that loss of the Phox subunit Cybb does not alter the growth or survival of *Mtb* during infection. Instead, *Cybb*$^{-/-}$ animals suffered from a hyper-inflammatory disease caused by increased activation of the NLRP3-dependent Caspase-1 inflammasome and IL-1-dependent neutrophil accumulation in the lung. Thus, the protective effect of Phox can be solely attributed to increased tolerance to *Mtb* infection instead of a direct antimicrobial effect. These studies provide a mechanism to explain the association between Phox expression and TB disease in natural populations, and implicate control of Caspase-1 activation as an important regulator of infection tolerance.

Materials and Methods

Mice

C57BL/6J (Stock # 000664), *Cybb*$^{-/-}$ (B6.129S-Cybb^{tm1Din}/J stock # 002365), Nos2$^{-/-}$ (B6.129P2-Nos2^{tm1Lau}/j, stock # 002609), B6.SJL-*Ptprc*^{a} *Pepc*^{b} carrying the pan leukocyte marker CD45.1 (stock # 002014) were purchased from the Jackson Laboratory. Mice were housed under specific pathogen-free conditions and in accordance with the University of Massachusetts Medical School, IACUC guidelines. All animals used for experiments were 6–12 weeks except mixed chimeras that were infected at 16 weeks following 8 weeks of reconstitution.

Mouse Infection

Wild type *M. tuberculosis* strain H37Rv was used for all studies unless indicated. This strain was confirmed to be PDIM-positive. Prior to infection bacteria were cultured in 7H9 medium containing 10% oleic albumin dextrose catalase growth supplement (OADC) enrichment (Becton Dickinson) and 0.05% Tween-80. H37Rv expressing sfYFP has been previously described and the episomal plasmid was maintained with selection in Hygromycin B (50ug/ml) added to the media (10). For low and high dose aerosol infections, bacteria were resuspended in phosphate-buffered saline containing Tween-80 (PBS-T). Prior to infection, bacteria were sonicated then delivered via the respiratory route using an aerosol generation device (Glas-Col). Infections of mice with the streptomycin dependent strain of *Mtb* (18b) have been previously described (36). In short, mice were infected via intra-tracheal infection and treated daily with 2mg of streptomycin daily for two weeks. For anti-IL1R treatment mice were injected with 200ug of anti-IL1R antibody or Isotype control (Bio-xcell) every other day starting at day 14. Both male and female mice were used throughout the study and no significant differences in phenotypes were observed between sexes.

Immunohistochemistry

Lungs from indicated mice were inflated with 10% buffered formalin and fixed for at least 24 hours then embedded in paraffin. Five-Micrometer—thick sections were stained with

hematoxylin and eosin (H&E). All staining was done by the Diabetes and Endocrinology Research Center Morphology Core at the University of Massachusetts Medical School.

Flow Cytometry

Lung tissue was harvested in DMEM containing FBS and placed in C-tubes (Miltenyi). Collagenase type IV/DNase I was added and tissues were dissociated for 10 seconds on a GentleMACS system (Miltenyi). Tissues were incubated for 30 minutes at 37°C with oscillations and then dissociated for an additional 30 seconds on a GentleMACS. Lung homogenates were passaged through a 70-micron filter or saved for subsequent analysis. Cell suspensions were washed in DMEM, passed through a 40-micron filter and aliquoted into 96 well plates for flow cytometry staining. Non-specific antibody binding was first blocked using Fc-Block. Cells were then stained with anti-Ly-6G Pacific Blue, anti-CD4 Pacific Blue, anti-CD11b PE, anti-CD11c APC, anti-Ly-6C APC-Cy7, anti-CD45.2 PercP Cy5.5, anti-CD3 FITC, anti-CD8 APC-Cy7, anti-B220 PE-Cy7 (Biolegend). Live cells were identified using fixable live dead aqua (Life Technologies). For infections with fluorescent H37Rv, lung tissue was prepared as above but no antibodies were used in the FITC channel. All of these experiments contained a non-fluorescent H37Rv infection control to identify infected cells. Cells were stained for 30 minutes at room temperature and fixed in 1% Paraformaldehyde for 60 minutes. All flow cytometry was run on a MACSQuant Analyzer 10 (Miltenyi) and was analyzed using FlowJo_V9 (Tree Star).

Macrophage and Dendritic Cell Generation

To generate bone marrow derived macrophages (BMDMs), marrow was isolated from femurs and tibia of age and sex matched mice. Cells were then incubated in DMEM (Sigma) containing 10% fetal bovine serum (FBS) and 20% L929 supernatant. Three days later media was exchanged with fresh media and seven days post-isolation cells were lifted with PBS-EDTA and seeded in DMEM containing 10% FBS for experiments.

To generate bone marrow derived dendritic cells (BMDCs), marrow was isolated from femurs and tibia of age- and sex-matched mice. Cell were then incubated in iMDM media (GIBCO) containing 10% FBS, L-Glutamine, 2μM 2-mercaptoethanol and 10% B16-GM-CSF supernatant (37). BMDCs were then purified on day six using Miltenyi LS columns first using negative selection for F480 followed by CD11c positive selection. Cells were then plated and infected the following day.

Macrophage and Dendritic Cell Infection

Mtb or *Mycobacterium bovis*-BCG were cultured in 7H9 medium containing 10% oleic albumin dextrose catalase growth supplement (OADC) enrichment (Becton Dickinson) and 0.05% Tween 80. Before infection cultures were washed in PBS-T, resuspended in DMEM containing 10%FBS and passed through a 5-micron filter to ensure single cells. Multiplicity of infection (MOI) was determined by optical density (OD) with an OD of 1 being equivalent to 3×10^8 bacteria per milliliter. Bacteria were added to macrophages for 4 hours then cells were washed with PBS and fresh media was added. At the indicated time points supernatants were harvested for cytokine analysis and the cells were processed for further analysis. Cell death was assessed using Cell-Titer-Glo luminescent cell viability assay

(Promega) following manufacturer's instructions. For inhibitor treatments cells were treated with the indicated concentrations of IFNγ (Peprotech), MCC950 (Adipogen) or VX-765 (Invivogen) or vehicle control overnight prior to infection and maintained in the media throughout the experiment.

Mixed Bone Marrow Chimera generation and cell sorting

Mixed bone marrow chimera experiments were done essentially as previously described (10). Wild type CD45.1^{+} mice were lethally irradiated with two doses of 600 rads. The following day, bone marrow from CD45.1^{+} wild-type mice and CD45.2^{+} knockout mice (wild type or Cybb$^{-/-}$) was isolated, red blood cells were lysed using Tris-buffered ammonium chloride (ACT), and the remaining cells were quantified using a haemocytometer. CD45.1^{+} and CD45.2^{+} cells were then mixed equally at a 1:1 ratio and 107 cells from this mixture were injected intravenously into lethally irradiated hosts that were placed on sulfatrim for three weeks. 8 weeks later mice were then infected by low-dose aerosol with *M. tuberculosis* H37Rv. Four weeks following infection, the lungs of chimera mice were processed for flow cytometry. An aliquot of this suspension was saved for flow cytometry analysis of the lung population and overall bacterial levels. The remaining cells were split equally and stained with either anti-CD45.1 APC or anti-CD45.2 PE. Stained populations were then incubated with either anti-APC or anti-PE magnetic beads (Miltenyi) following the manufacturer's instructions and sorted using LS-columns (Miltenyi). Purified cells were divided equally and then plated for *M. tuberculosis* on 7H10 agar or counted and stained for analysis of cellular purity. Cells from the input homogenate, flow through and the positive sort fractions were stained with for purity. Samples with >90% purity were used for subsequent analysis. At 21 days after plating, colonies were enumerated and the *Mtb* levels per sorted cells were determined.

qRT-PCR

Cells were lysed in Trizol-LS (Thermofisher), RNA was purified using Direct-zol RNA isolation kits (Zymogen) and quantified on nanodrop. RNA was diluted to 5ng/μl and 25 ng total RNA was used for each reaction. Ct values for each sample were determined in technical duplicates for β-Actin and IL-1β using one-step RT-PCR Kit (Qiagen) on a Viia7 Real-time PCR system (Life Technologies). ΔΔct values were then determined for each sample.

Immunoblotting, immunoblotting quantification and Cytokine quantification

Murine cytokine concentrations in culture supernatants and cell-free lung homogenates were quantified using commercial enzyme-linked immunosorbent assay (ELISA) kits (R&D). All samples were normalized for total protein content. Caspase1 activation in macrophage lysates was determined by western blotting with Caspase1 antibody purchased from Adipogen. Immunoblots were quantified using ImageJ software.

Results

Cybb$^{-/-}$ mice are susceptible to TB disease, but maintain control of bacterial replication.

In order to examine the role of Phox in mediating protection against *Mtb*, we compared disease progression and the immune responses in wild type and *Cybb*$^{-/-}$ C57BL/6 mice after infection via aerosol with 50–100 bacteria. We found no significant difference in the survival or bacterial levels in the lung between groups of mice up to 3 months following infection, confirming that Cybb is not required for surviving the early stages of *Mtb* infection (Figure 1A and S1). However, after 100 days of infection, *Cybb*$^{-/-}$ infected mice lost an average of 10% of their body weight while wild type animals gained weight (Figure 1B). Histopathological inspection of the lungs indicated a difference in disease between these groups, with *Cybb*$^{-/-}$ lungs containing larger and less organized lesions than wild type (Figure 1C). These data suggested that wild type and *Cybb*$^{-/-}$ animals might tolerate *Mtb* infection differently even while harboring identical levels of bacteria.

In order to dissect the mechanisms controlling tolerance to *Mtb* disease in *Cybb*$^{-/-}$ mice, we profiled the infected lungs of animals during infection by flow cytometry. We found no significant differences in the numbers of dendritic cells, macrophages, B cells, as well as total and activated T cells between wild type and *Cybb*$^{-/-}$ mice (Figure S1). In contrast, we observed an early and sustained increase of Ly6G^{+} CD11b^{+} neutrophils in the infected lungs of *Cybb*$^{-/-}$ mice (Figure 1D and 1E). A 3–5-fold increase in the total number neutrophils was observed as early as 4 weeks following infection and was maintained throughout the 12-week study.

The cytokine IL-1β promotes neutrophil-mediated disease during *Mtb* infection of other susceptible mouse strains (10, 36). Similarly, when we assayed cytokine levels in lung homogenates, we noted a dramatic and specific increase in IL-1β concentration in *Cybb*$^{-/-}$ animals compared to wild type at all time points (Figure 1F). In contrast, no significant differences were noted for IFNγ or TNFα at any time point between groups (Figure 1F). Thus, while the adaptive immune response to *Mtb* appeared to be intact, *Cybb*$^{-/-}$ animals produced excess IL-1β and the concentration of this cytokine correlated with neutrophil infiltration into the lung.

Previous studies have shown that following low dose aerosol infection mice deficient in Phox (both *Cybb*$^{-/-}$ or Ncf1$^{-/-}$) survive for at least 60 days (24, 25). However, longer infection is likely necessary to determine whether the enhanced disease we noted in *Cybb*$^{-/-}$ mice would result in a survival defect. These long-term survival experiments following low dose aerosol proved difficult, since uninfected *Cybb*$^{-/-}$ mice develop arthritis as they age (38). To avoid this confounder, we quantified the survival of mice in a shorter-term study using a high dose aerosol infection. When mice were infected with ~5000 CFU per animal, *Cybb*$^{-/-}$ mice succumbed to disease significantly more rapidly than wild type animals. *Cybb*$^{-/-}$ mice had a median survival time of 88 days while only two out of fifteen wild type mice succumbed during the 120-day study (Figure 1G). In order to distinguish survival effects not related to *Mtb* infection, a cohort of uninfected age-matched *Cybb*$^{-/-}$ mice were maintained for the duration of the experiment. None of these animals required euthanasia over the 120 days and no animals included in this experiment developed arthritis.

During this high-dose study, we also examined a cohort of mice 50 days following infection and found identical levels of bacteria in the lungs and spleen between wild type and *Cybb*$^{-/-}$ groups (Figure 1H). Consistent with our earlier findings, *Cybb*$^{-/-}$ mice showed a significant increase in neutrophils and IL-1β in the lung (Figure 1I-K). We also found minimal levels of IL-1β and neutrophils in uninfected *Cybb*$^{-/-}$ lungs indicating that these phenotypes are dependent on *Mtb* infection. Therefore, the loss of Cybb leads to more severe *Mtb* disease that is associated with increased IL-1β levels and neutrophil recruitment, even though the number of viable *Mtb* in the lung did not appear to be affected.

Cybb controls tolerance to *Mtb* infection.

Our initial results suggested that Cybb protects mice by promoting tolerance to *Mtb* infection rather than directly controlling bacterial replication. However, while viable bacterial numbers were similar in wild type and *Cybb*$^{-/-}$ mice, we could not rule out that the course of disease was altered by subtle changes in the dynamics of bacterial growth and death. To more rigorously address this question, we employed two additional animal models that allowed us to differentiate tolerance and direct antimicrobial resistance *in vivo*.

To more formally exclude the possibility that Cybb alters the intracellular growth of *Mtb* during infection, we used a previously optimized mixed bone marrow chimera approach (10). These experiments normalize potential inflammatory differences between wild type and *Cybb*$^{-/-}$ mice allowing us to specifically quantify differences in bacterial control (Figure 2A). Irradiated wild type mice were reconstituted with a 1:1 mixture of CD45.1^{+} wild type and CD45.2^{+} *Cybb*$^{-/-}$ or wild type cells. Five weeks following infection, both CD45.1^{+} and CD45.2^{+} cells were sorted from the lungs and the levels of *Mtb* in each genotype was determined by plating and the purity of populations was determined by flow cytometry (Figure 2B and 2C and Figure S2). We found that the relative abundance of wild type and *Cybb*$^{-/-}$ cells was similarly maintained throughout infection in both the myeloid and lymphoid compartments, indicating that Cybb does not alter cellular recruitment or survival in a cell-autonomous manner. When *Mtb* was enumerated in sorted cells, we found identical levels of H37Rv in wild type CD45.1^{+} and *Cybb*$^{-/-}$ CD45.2^{+} populations from the same mouse, similar to the results from mice where both populations were reconstituted with congenically mismatched wild type cells. In contrast, when chimeric mice were infected with a ROS-sensitive Δ*katG* mutant of *Mtb*, we found higher levels of bacteria in *Cybb*$^{-/-}$ cells compared to wild type cells from the same mouse. These data show that the assay is able to detect the cell-autonomous antimicrobial activity of ROS against a KatG-deficient *Mtb* strain, but Cybb-dependent ROS did not restrict the intracellular replication of wild type *Mtb*.

To specifically determine if the loss of Cybb decreased tolerance to a given burden of bacteria, wild type and *Cybb*$^{-/-}$ mice were infected with a streptomycin dependent strain of *Mtb* that allows exogenous control of bacterial replication during infection. Streptomycin is provided for the first two weeks of infection, allowing the pathogen to reach the burden observed in a wild type *Mtb* infection. Upon streptomycin withdrawal, the pathogen is unable to replicate but remains viable and able to drive inflammatory responses (Figure 2D) (10, 36, 39). Five weeks after infection, *Cybb*$^{-/-}$ mice lost more weight than wild type

animals while harboring identical levels of non-replicating bacteria (Figure 2E and2F). Lungs from *Cybb*$^{-/-}$ mice contained significantly more neutrophils and higher levels of IL-1β compared to wild type animals (Figure 2G-2I). Thus, even when the need for antimicrobial resistance is obviated by artificially inhibiting bacterial replication, *Cybb*$^{-/-}$ animals continued to exhibit a hyper-inflammatory disease.

The granulocytic inflammation observed in *Cybb*$^{-/-}$ mice was reminiscent of several other susceptible mouse strains. However, the neutrophil recruitment in other models is generally associated with a concomitant increase in bacterial growth (40–42) and a transition of the intracellular *Mtb* burden from macrophages to granulocytes (10). We hypothesized that *Cybb*$^{-/-}$ mice may be able to retain control of *Mtb* replication because the bacteria remain in macrophages. To test this hypothesis, we used a YFP-expressing *Mtb* strain to compare the distribution of cells harboring bacteria in wild type and *Cybb*$^{-/-}$ mice with *Nos2*$^{-/-}$ animals in which *Mtb* replicates to high numbers in association with infiltrating granulocytes (10). Four weeks following infection we found that lungs from both *Cybb*$^{-/-}$ and *Nos2*$^{-/-}$ mice contain higher levels of IL-1β and neutrophils than wild type animals, although the loss of *Nos2*$^{-/-}$ produced a much more severe phenotype than *Cybb*$^{-/-}$ (Figure 2J-2L and Figure S2). However, the cells harboring *Mtb* in these two susceptible mouse strains differed. In wild type and *Cybb*$^{-/-}$ mice, YFP-*Mtb* was evenly distributed between CD11b+/Ly6G+ neutrophils and the CD11b+/Ly6G- population that consists of macrophages and dendritic cells (43). This proportion was dramatically altered in *Nos2*$^{-/-}$ mice, where close to 90% of bacteria were found in the neutrophil compartment (Figure 2M and 2N). Thus, unlike other susceptible mouse models, the loss of Cybb does not alter bacterial replication or the distribution of *Mtb* in different myeloid subsets. Instead, this gene plays a specific role in controlling IL-1β activation, neutrophil recruitment to the infected lung, and disease progression. As a result, we conclude that Cybb specifically promotes tolerance to *Mtb* infection.

Enhanced IL-1β activation by *Cybb*$^{-/-}$ macrophages and dendritic cells is due to deregulated Caspase-1 inflammasome activation

To investigate the mechanism underlying increased IL-1β production in *Cybb*$^{-/-}$ mice, we quantified the release of mature cytokine from bone-marrow derived macrophages (BMDMs) and bone-marrow derived dendritic cells (BMDCs). Compared to wild type, we found that *Cybb*$^{-/-}$ BMDMs and BMDCs produced 4–5 fold more IL-1β after 24 hours of *Mtb* infection (Figure 3A and 3B). Under these conditions, wild type and *Cybb*$^{-/-}$ cells remained equally viable and produced equivalent amounts of TNF (Figure 3C-F), suggesting that the effect of Cybb on IL-1β activation was specific to this cytokine.

The release of mature IL-1β requires two distinct signals (44). The first signal induces the expression of *Il1b* mRNA and subsequent translation of pro-IL-1β, and a second signal activates Caspase 1, which is necessary for the processing and secretion of mature IL-1β. To understand what step of IL1β production was altered in *Cybb*$^{-/-}$ cells, we quantified these two signals. The expression of *Il1b* mRNA in uninfected and infected BMDMs was unchanged between wild type and *Cybb*$^{-/-}$ BMDMs (Figure 3G). In contrast, under the

same conditions, the processing of Caspase 1 to its active form was increased in infected *Cybb*$^{-/-}$ BMDMs compared to wild type cells (Figure 3H and 3I).

These observations suggested that caspase-1 activity is increased in *Cybb*$^{-/-}$ cells, which could allow mature IL-1β secretion in the absence of an inflammasome activator. To test this hypothesis, we stimulated cells with the TLR2 agonist, PAM3CSK4, to induce pro-IL-1β expression. PAM3CSK4 stimulation induced *Il1b* mRNA to similar levels between wild type and *Cybb*$^{-/-}$ BMDMs, albeit over 100 times higher than infection with *Mtb* (Figure 3J). In wild type cells, this induction of *Il1b* expression produced little mature IL-1β secretion, consistent with the need for subsequent inflammasome activation. In contrast, induction of *Il1b* expression led to robust secretion of mature IL-1β from *Cybb*$^{-/-}$ BMDM, consistent with unregulated inflammasome activity in these cells (Figure 3K). Together these data show that loss of Cybb leads to hyper-activation of Caspase1 and increased release of IL-1β during *Mtb* infection of both BMDMs and BMDCs.

Loss of tolerance is reversed in *Cybb*$^{-/-}$ macrophages and mice by blocking the production or activity of IL-1β

The NLRP3 inflammasome consists of NLRP3, ASC, and Caspase 1. While this complex is generally responsible for IL-1β processing in *Mtb* infected macrophages (45, 46), it remained unclear whether the enhanced IL-1β secretion from *Cybb*$^{-/-}$ cells also relied on these components. To identify the responsible complex, we blocked the activation of the NLRP3 inflammasome in several distinct ways. The NLRP3 inflammasome is specifically inhibited by IFNγ stimulation, via the nitric oxide-dependent nitrosylation of the NLRP3 protein (36). Pretreatment of wild type and *Cybb*$^{-/-}$ BMDMs with varying concentrations of IFNγ, inhibited the secretion of mature IL-1β from both wild type and *Cybb*$^{-/-}$ BMDMs compared to untreated cells. While this result indicated an important role for NLRP3, IFNγ pretreatment did not completely suppress IL-1β secretion and there remained significant differences in the IL-1β release between *Cybb*$^{-/-}$ and wild type cells at all concentrations of the cytokine (Figure 4A).

To more directly assess the role of NLRP3 and Caspase-1 in IL-1β maturation in *Cybb*$^{-/-}$ cells, we employed specific small molecule inhibitors. Treatment of *Mtb*-infected BMDMs with either the NLRP3 inhibitor, MCC950 (45), or the Caspase-1 inhibitor, VX-765 (47) caused a dramatic reduction in IL-1β in both wild type and *Cybb*$^{-/-}$ BMDMs compared to untreated cells (Figure 4B and 4C). This ten-fold decrease in IL-1β secretion could not be attributed to inhibition of pro-IL-1β levels, as none of these inhibitors affected *Il1b* mRNA by more than two-fold. Similarly, the spontaneous IL-1β secretion observed upon PAM3CSK4 stimulation was also inhibited by MCC950 and IFNγ (Figure 4E). In each case, inflammasome inhibition reduced IL-1β secretion to the same level in both wild type and *Cybb*$^{-/-}$ cells, indicating that the NLRP3 inflammasome was responsible for the enhanced processing and secretion of this cytokine in *Cybb*$^{-/-}$ BMDM.

Based on these studies, we hypothesized that the tolerance defect observed in the intact mouse was due to inflammasome-dependent IL-1 signaling. The contributions of IL-1β during *Mtb* infection are complex (48, 49). Production of this cytokine is important for antimicrobial immunity, but persistent IL-1 signaling can promote pathology. In order to

focus on the role of over-production of IL-1β on tolerance, we inhibited IL-1 signaling in mice infected with non-replicating streptomycin-dependent *Mtb* to normalize the bacterial burden. Two weeks after infection, wild type and $Cybb^{-/-}$ mice were treated with either an isotype control antibody or an anti-IL1R antibody to block the effect of increased IL-1β activity. As expected, *Mtb* levels were similar in all mice, but more neutrophils accumulated in the lungs $Cybb^{-/-}$ animals (Figure 4F-H). While anti-IL-1R treatment had no effect in wild type animals, inhibition of IL-1 signaling reduced neutrophil infiltration in $Cybb^{-/-}$ mice to the level observed in wild type animals. Taken together, our data show that $Cybb^{-/-}$ contributes to protective immunity to *Mtb* not by controlling bacterial replication, but instead by preventing an IL-1-dependent inflammatory response that increases neutrophil recruitment to the lung and exacerbates disease progression.

Discussion

The role of the Phox complex in protection from TB has presented a paradox (34). Based on the well-described antimicrobial properties of Phox-derived ROS, previous studies have focused on examining the function of Phox components in controlling *Mtb* replication in mice (24, 25, 50). The lack of a long-term differences in bacterial levels observed in these studies suggested that Phox may not play a strong antimicrobial role during *Mtb* infection. Our dissection of disease progression in Cybb-deficient mice shows that Phox plays no discernable role in antimicrobial resistance to *Mtb* over long-term infections. However, we uncovered a previously unknown role for this complex in promoting tolerance to *Mtb* infection and inhibiting TB disease.

While we were able to clearly delineate the role of Phox during *Mtb* infection, the role(s) played by this complex in any given infection is likely to vary. Phox-deficient mice are unable to control the growth of several bacterial pathogens that are known to cause serious infections in CGD patients, including non-tuberculous mycobacteria (50–53). In the context of these infections, the antimicrobial functions of Phox may predominate. In fact, several studies suggest an important role for Phox in controlling replication of pathogenic mycobacteria other than *Mtb*. High-dose intravenous or intratracheal infection with *M. avium, M. marinum*, and *M. bovis* BCG all produce higher bacterial burdens and more severe disease in Phox-deficient mice than wild type animals (50, 53, 54). While these observations indicate that Phox can play an antimicrobial role in these infections, the specific role of this complex in promoting tolerance could not be discerned due to the difference in bacterial numbers in wild type and mutant animals.

The differential dependency on Phox for antimicrobial resistance to *Mtb* versus these other mycobacterial species likely reflects a differential susceptibility to ROS-mediated killing. Several studies support this model by demonstrating that mechanisms by which neutrophils kill these different organisms are distinct. Neutrophil-mediated killing of *Mtb* is independent of Phox derived ROS, as neutrophils from CGD-patients show no defect in *Mtb* killing and inhibitors of ROS do not alter this activity (55, 56). In contrast, *M. marinum* is killed by neutrophils in a ROS-dependent manner (57). Similarly, neutrophil depletion promotes the growth of BCG in the lung but has little effect in the context of *Mtb* (10, 58). This effect can be explained based on the ability of the ESX-1 secretion system, which is absent from BCG,

to inhibit neutrophil killing (59). Based on these differences in susceptibility to neutrophil killing, we speculate that Phox-derived ROS may contribute to both tolerance and resistance to mycobacteria, such as *M. avium* or *M. bovis* BCG, but this remains to be rigorously tested. For a pathogen such as *Mtb* that is resistant to ROS-mediated toxicity and persists in the tissue to promote continual inflammatory damage, the tolerance-promoting activity of Phox predominates.

During *Mtb* infection, we found that the ROS produced by Phox are critical to control the activation of the NLRP3 inflammasome. In contrast, mitochondrial ROS are well known to activate inflammatory cascades (60), suggesting that the context by which ROS are produced influences the inflammatory outcome of activated cells. Despite this complexity, Phox-deficient mice and CGD patients suffer from hyper-inflammatory diseases including arthritis, colitis, and prolonged inflammatory reactions to microbial products, indicating that the dominant immunoregulatory role for Phox-derived ROS is anti-inflammatory (61–63). While the noninfectious granulomatous lesions of CGD patients are typified by mononuclear infiltrate, the histopathology of infectious foci are more variable. Pulmonary infections generally produce either pneumonia or abscess, which might resemble the neutrophil-associated disease that we observe in mice (64).

CGD patients are more likely to develop disseminated BCG infections following vaccination. While it is likely *M. bovis* is differentially susceptible to ROS killing as discussed above it is also possible enhanced inflammasome activation contributes to this disease. While inflammasome activation in wild type animals requires the ESX-1 secretion system that is deleted in BCG, we observed robust stimulation of inflammasome activation in Phox deficient cells treated with TLR stimulation alone. These results suggest that activation of Caspase1 may occur in Phox-deficient cells even upon infection with ESX-1 deficient pathogens.

Several non-mutually exclusive mechanisms could explain the anti-inflammatory effect of Phox-derived ROS. For example, ROS has been proposed to inhibit the production of inflammatory mediators by inhibiting autophagy (65). In the absence of ROS, the reduced levels of autophagy may drive enhanced inflammasome activation. Another mechanism was described in superoxide dismutase1 (*Sod1*) deficient cells, where the accumulation of ROS inhibits Caspase1 activation through glutathionation of reactive cysteines (66). It is possible that the loss of ROS leads to loss of glutathionation and subsequently results in the hyper-activation of Caspase1. This latter mechanism is reminiscent of the process by which nitric oxide (NO), inhibits inflammasome activation via S-nitrosylation of NLRP3 (36). The intersection of these two important anti-inflammatory pathways at the NLRP3 inflammasome indicates that this complex may be a critical point of integration where inflammatory cascades are controlled during chronic infections.

Our findings are consistent with a growing body of literature suggesting that inflammasome-derived IL-1 promotes TB disease progression. For example, genetic polymorphisms that increase the expression of IL1β or the production of IL-1 dependent pro-inflammatory lipid mediators are associated with TB disease progression (10, 67). Similarly, transcriptional signatures of inflammasome activation have been observed in severe forms of TB disease,

such as meningitis (68) and TB-associated immune reconstitution syndrome (69). Together with our work, these finding imply that a failure in tolerance alone can compromise protective immunity to *Mtb*, even in the context of fully functional antimicrobial resistance responses, and that Caspase-1 represents a critical point at which tolerance is regulated.

Supplementary Material

Refer to Web version on PubMed Central for supplementary material.

Acknowledgements

We are thankful to members of the Sassetti, Behar and Fitzgerald lab for helpful discussions. This work was funded by the Arnold and Mabel Beckman Postdoctoral Fellowship (AO), Charles King Trust Postdoctoral Fellowship (CMSmith), and NIH Grant AI132130 (CMSassetti)

References

1. Medzhitov R, Schneider DS, and Soares MP. 2012 Disease tolerance as a defense strategy. Science 335: 936–941. [PubMed: 22363001]
2. Schneider DS, and Ayres JS. 2008 Two ways to survive infection: what resistance and tolerance can teach us about treating infectious diseases. Nat Rev Immunol 8: 889–895. [PubMed: 18927577]
3. Olive AJ, and Sassetti CM. 2016 Metabolic crosstalk between host and pathogen: sensing, adapting and competing. Nat Rev Microbiol 14: 221–234. [PubMed: 26949049]
4. Pilla-Moffett D, Barber MF, Taylor GA, and Coers J. 2016 Interferon-Inducible GTPases in Host Resistance, Inflammation and Disease. J Mol Biol 428: 3495–3513. [PubMed: 27181197]
5. Hood MI, and Skaar EP. 2012 Nutritional immunity: transition metals at the pathogen-host interface. Nat Rev Microbiol 10: 525–537. [PubMed: 22796883]
6. Ayres JS, and Schneider DS. 2008 A signaling protease required for melanization in Drosophila affects resistance and tolerance of infections. PLoS Biol 6: 2764–2773. [PubMed: 19071960]
7. Weis S, Carlos AR, Moita MR, Singh S, Blankenhaus B, Cardoso S, Larsen R, Rebelo S, Schauble S, Del Barrio L, Mithieux G, Rajas F, Lindig S, Bauer M, and Soares MP. 2017 Metabolic Adaptation Establishes Disease Tolerance to Sepsis. Cell 169: 1263–1275 e1214. [PubMed: 28622511]
8. Jamieson AM, Pasman L, Yu S, Gamradt P, Homer RJ, Decker T, and Medzhitov R. 2013 Role of tissue protection in lethal respiratory viral-bacterial coinfection. Science 340: 1230–1234. [PubMed: 23618765]
9. Jeney V, Ramos S, Bergman ML, Bechmann I, Tischer J, Ferreira A, Oliveira-Marques V, Janse CJ, Rebelo S, Cardoso S, and Soares MP. 2014 Control of disease tolerance to malaria by nitric oxide and carbon monoxide. Cell Rep 8: 126–136. [PubMed: 24981859]
10. Mishra BB, Lovewell RR, Olive AJ, Zhang G, Wang W, Eugenin E, Smith CM, Phuah JY, Long JE, Dubuke ML, Palace SG, Goguen JD, Baker RE, Nambi S, Mishra R, Booty MG, Baer CE, Shaffer SA, Dartois V, McCormick BA, Chen X, and Sassetti CM. 2017 Nitric oxide prevents a pathogen-permissive granulocytic inflammation during tuberculosis. Nat Microbiol 2: 17072. [PubMed: 28504669]
11. Meunier I, Kaufmann E, Downey J, and Divangahi M. 2017 Unravelling the networks dictating host resistance versus tolerance during pulmonary infections. Cell Tissue Res 367: 525–536. [PubMed: 28168323]
12. Cadena AM, Fortune SM, and Flynn JL. 2017 Heterogeneity in tuberculosis. Nat Rev Immunol
13. Chen RY, Dodd LE, Lee M, Paripati P, Hammoud DA, Mountz JM, Jeon D, Zia N, Zahiri H, Coleman MT, Carroll MW, Lee JD, Jeong YJ, Herscovitch P, Lahouar S, Tartakovsky M, Rosenthal A, Somaiyya S, Lee S, Goldfeder LC, Cai Y, Via LE, Park SK, Cho SN, and Barry CE, 3rd. 2014 PET/CT imaging correlates with treatment outcome in patients with multidrug-resistant tuberculosis. Sci Transl Med 6: 265ra166.

14. Tobin DM, Roca FJ, Oh SF, McFarland R, Vickery TW, Ray JP, Ko DC, Zou Y, Bang ND, Chau TT, Vary JC, Hawn TR, Dunstan SJ, Farrar JJ, Thwaites GE, King MC, Serhan CN, and Ramakrishnan L. 2012 Host genotype-specific therapies can optimize the inflammatory response to mycobacterial infections. Cell 148: 434–446. [PubMed: 22304914]
15. Lopez B, Aguilar D, Orozco H, Burger M, Espitia C, Ritacco V, Barrera L, Kremer K, Hernandez-Pando R, Huygen K, and van Soolingen D. 2003 A marked difference in pathogenesis and immune response induced by different Mycobacterium tuberculosis genotypes. Clin Exp Immunol 133: 30–37. [PubMed: 12823275]
16. Redford PS, Murray PJ, and O'Garra A. 2011 The role of IL-10 in immune regulation during M. tuberculosis infection. Mucosal Immunol 4: 261–270. [PubMed: 21451501]
17. Larson RP, Shafiani S, and Urdahl KB. 2013 Foxp3(+) regulatory T cells in tuberculosis. Adv Exp Med Biol 783: 165–180. [PubMed: 23468109]
18. Jayaraman P, Jacques MK, Zhu C, Steblenko KM, Stowell BL, Madi A, Anderson AC, Kuchroo VK, and Behar SM. 2016 TIM3 Mediates T Cell Exhaustion during Mycobacterium tuberculosis Infection. PLoS Pathog 12: e1005490. [PubMed: 26967901]
19. Desvignes L, Weidinger C, Shaw P, Vaeth M, Ribierre T, Liu M, Fergus T, Kozhaya L, McVoy L, Unutmaz D, Ernst JD, and Feske S. 2015 STIM1 controls T cell-mediated immune regulation and inflammation in chronic infection. J Clin Invest 125: 2347–2362. [PubMed: 25938788]
20. Pasipanodya JG, McNabb SJ, Hilsenrath P, Bae S, Lykens K, Vecino E, Munguia G, Miller TL, Drewyer G, and Weis SE. 2010 Pulmonary impairment after tuberculosis and its contribution to TB burden. BMC Public Health 10: 259. [PubMed: 20482835]
21. Segal AW 2005 How neutrophils kill microbes. Annu Rev Immunol 23: 197–223. [PubMed: 15771570]
22. Panday A, Sahoo MK, Osorio D, and Batra S. 2015 NADPH oxidases: an overview from structure to innate immunity-associated pathologies. Cell Mol Immunol 12: 5–23. [PubMed: 25263488]
23. Johnston RB, Jr., and Baehner RL. 1970 Improvement of leukocyte bactericidal activity in chronic granulomatous disease. Blood 35: 350–355. [PubMed: 4908653]
24. Cooper AM, Segal BH, Frank AA, Holland SM, and Orme IM. 2000 Transient loss of resistance to pulmonary tuberculosis in p47(phox−/−) mice. Infect Immun 68: 1231–1234. [PubMed: 10678931]
25. Jung YJ, LaCourse R, Ryan L, and North RJ. 2002 Virulent but not avirulent Mycobacterium tuberculosis can evade the growth inhibitory action of a T helper 1-dependent, nitric oxide Synthase 2-independent defense in mice. J Exp Med 196: 991–998. [PubMed: 12370260]
26. Ng VH, Cox JS, Sousa AO, MacMicking JD, and McKinney JD. 2004 Role of KatG catalase-peroxidase in mycobacterial pathogenesis: countering the phagocyte oxidative burst. Mol Microbiol 52: 1291–1302. [PubMed: 15165233]
27. Colangeli R, Haq A, Arcus VL, Summers E, Magliozzo RS, McBride A, Mitra AK, Radjainia M, Khajo A, Jacobs WR, Jr., Salgame P, and Alland D. 2009 The multifunctional histone-like protein Lsr2 protects mycobacteria against reactive oxygen intermediates. Proc Natl Acad Sci U S A 106: 4414–4418. [PubMed: 19237572]
28. Nambi S, Long JE, Mishra BB, Baker R, Murphy KC, Olive AJ, Nguyen HP, Shaffer SA, and Sassetti CM. 2015 The Oxidative Stress Network of Mycobacterium tuberculosis Reveals Coordination between Radical Detoxification Systems. Cell Host Microbe 17: 829–837. [PubMed: 26067605]
29. Koster S, Upadhyay S, Chandra P, Papavinasasundaram K, Yang G, Hassan A, Grigsby SJ, Mittal E, Park HS, Jones V, Hsu FF, Jackson M, Sassetti CM, and Philips JA. 2017 Mycobacterium tuberculosis is protected from NADPH oxidase and LC3-associated phagocytosis by the LCP protein CpsA. Proc Natl Acad Sci U S A 114: E8711–E8720. [PubMed: 28973896]
30. Nathan C, and Shiloh MU. 2000 Reactive oxygen and nitrogen intermediates in the relationship between mammalian hosts and microbial pathogens. Proc Natl Acad Sci U S A 97: 8841–8848. [PubMed: 10922044]
31. Bustamante J, Arias AA, Vogt G, Picard C, Galicia LB, Prando C, Grant AV, Marchal CC, Hubeau M, Chapgier A, de Beaucoudrey L, Puel A, Feinberg J, Valinetz E, Janniere L, Besse C, Boland A, Brisseau JM, Blanche S, Lortholary O, Fieschi C, Emile JF, Boisson-Dupuis S, Al-Muhsen S,

Woda B, Newburger PE, Condino-Neto A, Dinauer MC, Abel L, and Casanova JL. 2011 Germline CYBB mutations that selectively affect macrophages in kindreds with X-linked predisposition to tuberculous mycobacterial disease. Nat Immunol 12: 213–221. [PubMed: 21278736]

32. Khan TA, Kalsoom K, Iqbal A, Asif H, Rahman H, Farooq SO, Naveed H, Nasir U, Amin MU, Hussain M, Tipu HN, and Florea A. 2016 A novel missense mutation in the NADPH binding domain of CYBB abolishes the NADPH oxidase activity in a male patient with increased susceptibility to infections. Microb Pathog 100: 163–169. [PubMed: 27666509]
33. Lee PP, Chan KW, Jiang L, Chen T, Li C, Lee TL, Mak PH, Fok SF, Yang X, and Lau YL. 2008 Susceptibility to mycobacterial infections in children with X-linked chronic granulomatous disease: a review of 17 patients living in a region endemic for tuberculosis. Pediatr Infect Dis J 27: 224–230. [PubMed: 18277931]
34. Deffert C, Cachat J, and Krause KH. 2014 Phagocyte NADPH oxidase, chronic granulomatous disease and mycobacterial infections. Cell Microbiol 16: 1168–1178. [PubMed: 24916152]
35. Lau YL, Chan GC, Ha SY, Hui YF, and Yuen KY. 1998 The role of phagocytic respiratory burst in host defense against Mycobacterium tuberculosis. Clin Infect Dis 26: 226–227. [PubMed: 9455564]
36. Mishra BB, Rathinam VA, Martens GW, Martinot AJ, Kornfeld H, Fitzgerald KA, and Sassetti CM. 2013 Nitric oxide controls the immunopathology of tuberculosis by inhibiting NLRP3 inflammasome-dependent processing of IL-1beta. Nat Immunol 14: 52–60. [PubMed: 23160153]
37. Zanoni I, Tan Y, Di Gioia M, Broggi A, Ruan J, Shi J, Donado CA, Shao F, Wu H, Springstead JR, and Kagan JC. 2016 An endogenous caspase-11 ligand elicits interleukin-1 release from living dendritic cells. Science 352: 1232–1236. [PubMed: 27103670]
38. Lee K, Won HY, Bae MA, Hong JH, and Hwang ES. 2011 Spontaneous and aging-dependent development of arthritis in NADPH oxidase 2 deficiency through altered differentiation of CD11b + and Th/Treg cells. Proc Natl Acad Sci U S A 108: 9548–9553. [PubMed: 21593419]
39. Honore N, Marchal G, and Cole ST. 1995 Novel mutation in 16S rRNA associated with streptomycin dependence in Mycobacterium tuberculosis. Antimicrob Agents Chemother 39: 769–770. [PubMed: 7540819]
40. Kimmey JM, Huynh JP, Weiss LA, Park S, Kambal A, Debnath J, Virgin HW, and Stallings CL. 2015 Unique role for ATG5 in neutrophil-mediated immunopathology during M. tuberculosis infection. Nature 528: 565–569. [PubMed: 26649827]
41. Kramnik I, Dietrich WF, Demant P, and Bloom BR. 2000 Genetic control of resistance to experimental infection with virulent Mycobacterium tuberculosis. Proc Natl Acad Sci U S A 97: 8560–8565. [PubMed: 10890913]
42. Nandi B, and Behar SM. 2011 Regulation of neutrophils by interferon-gamma limits lung inflammation during tuberculosis infection. J Exp Med 208: 2251–2262. [PubMed: 21967766]
43. Wolf AJ, Linas B, Trevejo-Nunez GJ, Kincaid E, Tamura T, Takatsu K, and Ernst JD. 2007 Mycobacterium tuberculosis infects dendritic cells with high frequency and impairs their function in vivo. J Immunol 179: 2509–2519. [PubMed: 17675513]
44. von Moltke J, Ayres JS, Kofoed EM, Chavarria-Smith J, and Vance RE. 2013 Recognition of bacteria by inflammasomes. Annu Rev Immunol 31: 73–106. [PubMed: 23215645]
45. Coll RC, Robertson AA, Chae JJ, Higgins SC, Munoz-Planillo R, Inserra MC, Vetter I, Dungan LS, Monks BG, Stutz A, Croker DE, Butler MS, Haneklaus M, Sutton CE, Nunez G, Latz E, Kastner DL, Mills KH, Masters SL, Schroder K, Cooper MA, and O'Neill LA. 2015 A small-molecule inhibitor of the NLRP3 inflammasome for the treatment of inflammatory diseases. Nat Med 21: 248–255. [PubMed: 25686105]
46. Dorhoi A, Nouailles G, Jorg S, Hagens K, Heinemann E, Pradl L, Oberbeck-Muller D, Duque-Correa MA, Reece ST, Ruland J, Brosch R, Tschopp J, Gross O, and Kaufmann SH. 2012 Activation of the NLRP3 inflammasome by Mycobacterium tuberculosis is uncoupled from susceptibility to active tuberculosis. Eur J Immunol 42: 374–384. [PubMed: 22101787]
47. Stack JH, Beaumont K, Larsen PD, Straley KS, Henkel GW, Randle JC, and Hoffman HM. 2005 IL-converting enzyme/caspase-1 inhibitor VX-765 blocks the hypersensitive response to an inflammatory stimulus in monocytes from familial cold autoinflammatory syndrome patients. J Immunol 175: 2630–2634. [PubMed: 16081838]

48. Mayer-Barber KD, Barber DL, Shenderov K, White SD, Wilson MS, Cheever A, Kugler D, Hieny S, Caspar P, Nunez G, Schlueter D, Flavell RA, Sutterwala FS, and Sher A. 2010 Caspase-1 independent IL-1beta production is critical for host resistance to mycobacterium tuberculosis and does not require TLR signaling in vivo. J Immunol 184: 3326–3330. [PubMed: 20200276]
49. Nunes-Alves C, Booty MG, Carpenter SM, Jayaraman P, Rothchild AC, and Behar SM. 2014 In search of a new paradigm for protective immunity to TB. Nat Rev Microbiol 12: 289–299. [PubMed: 24590243]
50. Deffert C, Schappi MG, Pache JC, Cachat J, Vesin D, Bisig R, Ma Mulone X, Kelkka T, Holmdahl R, Garcia I, Olleros ML, and Krause KH. 2014 Bacillus calmette-guerin infection in NADPH oxidase deficiency: defective mycobacterial sequestration and granuloma formation. PLoS Pathog 10: e1004325. [PubMed: 25188296]
51. Jackson SH, Gallin JI, and Holland SM. 1995 The p47phox mouse knock-out model of chronic granulomatous disease. J Exp Med 182: 751–758. [PubMed: 7650482]
52. Dinauer MC, Deck MB, and Unanue ER. 1997 Mice lacking reduced nicotinamide adenine dinucleotide phosphate oxidase activity show increased susceptibility to early infection with Listeria monocytogenes. J Immunol 158: 5581–5583. [PubMed: 9190903]
53. Fujita M, Harada E, Matsumoto T, Mizuta Y, Ikegame S, Ouchi H, Inoshima I, Yoshida S, Watanabe K, and Nakanishi Y. 2010 Impaired host defence against Mycobacterium avium in mice with chronic granulomatous disease. Clin Exp Immunol 160: 457–460. [PubMed: 20089078]
54. Chao WC, Yen CL, Hsieh CY, Huang YF, Tseng YL, Nigrovic PA, and Shieh CC. 2017 Mycobacterial infection induces higher interleukin-1beta and dysregulated lung inflammation in mice with defective leukocyte NADPH oxidase. PLoS One 12: e0189453. [PubMed: 29228045]
55. Jones GS, Amirault HJ, and Andersen BR. 1990 Killing of Mycobacterium tuberculosis by neutrophils: a nonoxidative process. J Infect Dis 162: 700–704. [PubMed: 2167338]
56. Kisich KO, Higgins M, Diamond G, and Heifets L. 2002 Tumor necrosis factor alpha stimulates killing of Mycobacterium tuberculosis by human neutrophils. Infect Immun 70: 4591–4599. [PubMed: 12117972]
57. Yang CT, Cambier CJ, Davis JM, Hall CJ, Crosier PS, and Ramakrishnan L. 2012 Neutrophils exert protection in the early tuberculous granuloma by oxidative killing of mycobacteria phagocytosed from infected macrophages. Cell Host Microbe 12: 301–312. [PubMed: 22980327]
58. Fulton SA, Reba SM, Martin TD, and Boom WH. 2002 Neutrophil-mediated mycobacteriocidal immunity in the lung during Mycobacterium bovis BCG infection in C57BL/6 mice. Infect Immun 70: 5322–5327. [PubMed: 12183593]
59. Francis RJ, Butler RE, and Stewart GR. 2014 Mycobacterium tuberculosis ESAT-6 is a leukocidin causing Ca2+ influx, necrosis and neutrophil extracellular trap formation. Cell Death Dis 5: e1474. [PubMed: 25321481]
60. Weinberg SE, Sena LA, and Chandel NS. 2015 Mitochondria in the regulation of innate and adaptive immunity. Immunity 42: 406–417. [PubMed: 25786173]
61. Segal BH, Han W, Bushey JJ, Joo M, Bhatti Z, Feminella J, Dennis CG, Vethanayagam RR, Yull FE, Capitano M, Wallace PK, Minderman H, Christman JW, Sporn MB, Chan J, Vinh DC, Holland SM, Romani LR, Gaffen SL, Freeman ML, and Blackwell TS. 2010 NADPH oxidase limits innate immune responses in the lungs in mice. PLoS One 5: e9631. [PubMed: 20300512]
62. Morgenstern DE, Gifford MA, Li LL, Doerschuk CM, and Dinauer MC. 1997 Absence of respiratory burst in X-linked chronic granulomatous disease mice leads to abnormalities in both host defense and inflammatory response to Aspergillus fumigatus. J Exp Med 185: 207–218. [PubMed: 9016870]
63. Schappi M, Deffert C, Fiette L, Gavazzi G, Herrmann F, Belli D, and Krause KH. 2008 Branched fungal beta-glucan causes hyperinflammation and necrosis in phagocyte NADPH oxidase-deficient mice. J Pathol 214: 434–444. [PubMed: 18098349]
64. van den Berg JM, van Koppen E, Ahlin A, Belohradsky BH, Bernatowska E, Corbeel L, Espanol T, Fischer A, Kurenko-Deptuch M, Mouy R, Petropoulou T, Roesler J, Seger R, Stasia MJ, Valerius NH, Weening RS, Wolach B, Roos D, and Kuijpers TW. 2009 Chronic granulomatous disease: the European experience. PLoS One 4: e5234. [PubMed: 19381301]

65. de Luca A, Smeekens SP, Casagrande A, Iannitti R, Conway KL, Gresnigt MS, Begun J, Plantinga TS, Joosten LA, van der Meer JW, Chamilos G, Netea MG, Xavier RJ, Dinarello CA, Romani L, and van de Veerdonk FL. 2014 IL-1 receptor blockade restores autophagy and reduces inflammation in chronic granulomatous disease in mice and in humans. Proc Natl Acad Sci U S A 111: 3526–3531. [PubMed: 24550444]

66. Meissner F, Molawi K, and Zychlinsky A. 2008 Superoxide dismutase 1 regulates caspase-1 and endotoxic shock. Nat Immunol 9: 866–872. [PubMed: 18604212]

67. Zhang G, Zhou B, Li S, Yue J, Yang H, Wen Y, Zhan S, Wang W, Liao M, Zhang M, Zeng G, Feng CG, Sassetti CM, and Chen X. 2014 Allele-specific induction of IL-1beta expression by C/EBPbeta and PU.1 contributes to increased tuberculosis susceptibility. PLoS Pathog 10: e1004426. [PubMed: 25329476]

68. Marais S, Lai RPJ, Wilkinson KA, Meintjes G, O'Garra A, and Wilkinson RJ. 2017 Inflammasome Activation Underlying Central Nervous System Deterioration in HIV-Associated Tuberculosis. J Infect Dis 215: 677–686. [PubMed: 27932622]

69. Tan HY, Yong YK, Shankar EM, Paukovics G, Ellegard R, Larsson M, Kamarulzaman A, French MA, and Crowe SM. 2016 Aberrant Inflammasome Activation Characterizes Tuberculosis-Associated Immune Reconstitution Inflammatory Syndrome. J Immunol 196: 4052–4063.. [PubMed: 27076678] .

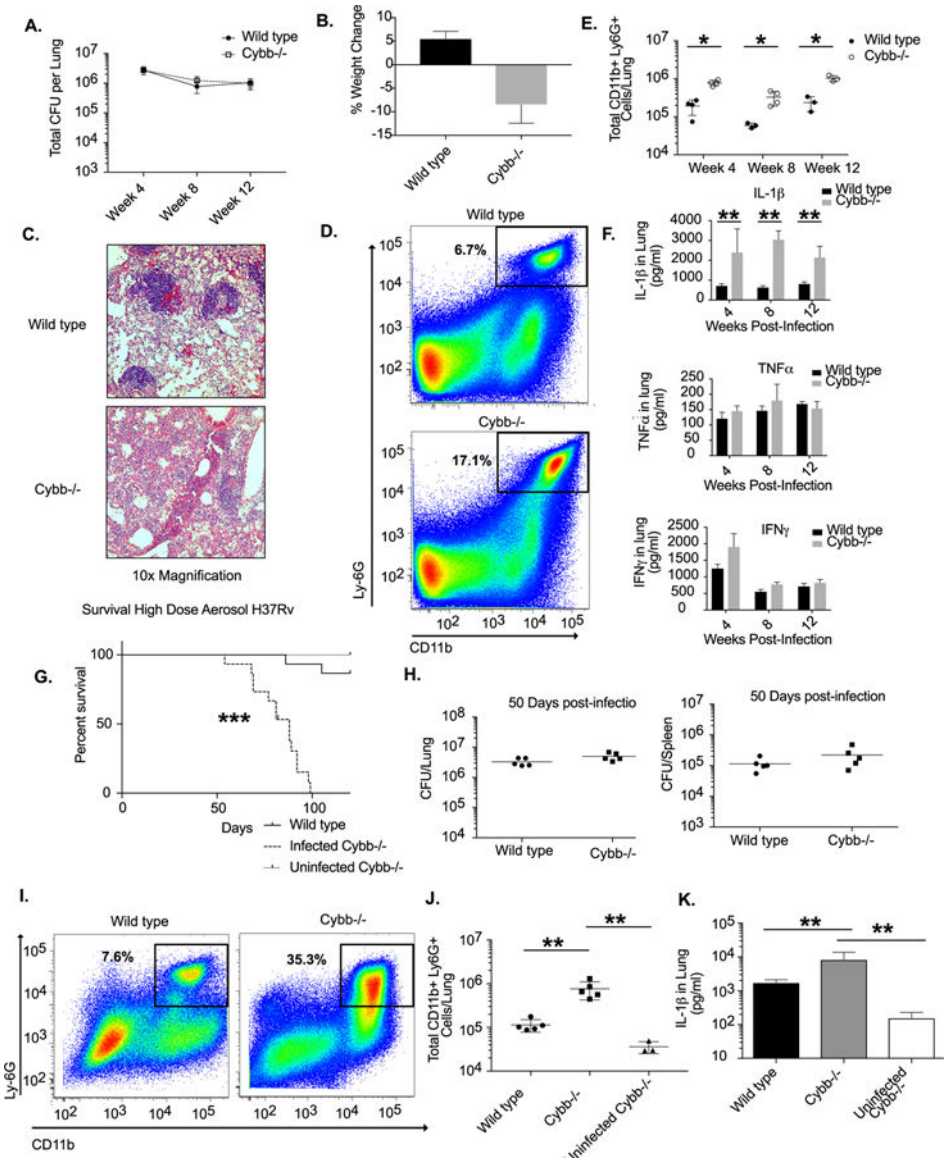

Figure 1. Anti-inflammatory activity of Cybb protects mice from TB disease.

A. Following low dose aerosol infection (Day 20 of ~50–100 colony forming units, cfu) total bacterial burden (expressed in cfu, mean $^{+/-}$ s.d.) was determined in the lungs of wild type or *Cybb*$^{-/-}$ mice at the indicated time points with 4–5 mice per group. **B.** Percentage weight loss (mean change $^{+/-}$ s.d) from Day 30 to Day 100 was determined for wild type and *Cybb* $^{-/-}$ mice. Representative of two experiments with 3–5 mice per group. **C.** Immunohistochemical staining for Haemotoxylin and Eosin is shown for representative lung sections from wild type and *Cybb*$^{-/-}$ mice at 48 weeks post-infection at 20x magnification. **D.** Representative flow cytometry plot showing increased Ly56G^{+} CD11b^{+} neutrophil recruitment to the lungs of *Cybb*$^{-/-}$ mice 4 weeks following infection (gated on live/singlets/ CD45^{+}). **E.** Quantification of neutrophil recruitment to the lungs at the indicated time points following infection for wild type and *Cybb*$^{-/-}$ mice is shown as absolute number of Ly66G^{+} CD11b^{+} cells per lung (mean $^{+/-}$ s.d). * p-value <.05 by unpaired two-tailed t-test.

Representative of 4 experiments with 3–5 mice per group. **F.** Lung homogenates from wild type or *Cybb*$^{-/-}$ mice infected for the indicated time were probed for the cytokines IL-71β, IFNγ, and TNFα by ELISA (mean $^{+/-}$ s.d). Results shown in A-D are representative of 3 independent experiments with 3–5 mice per group. ** p-value <.01 by unpaired two-tailed t-test. **G.** Survival of infected wild type and *Cybb*$^{-/-}$ and uninfected *Cybb*$^{-/-}$ mice was determined following high dose infection. Data are representative of two independent experiments with 814–15 mice per group. *** p-value <.001 Mantel-Cox text. **H.** Fifty days following high dose aerosol infection (Day 90 of 5000–7500 CFU) total bacterial burden (expressed in cfu, mean $^{+/-}$ s.d.) was determined in the lungs and spleen of wild type or *Cybb*$^{-/-}$ mice. Data are representative of two experiments 4–5 mice per group. **I.** Representative flow cytometry plot showing increased Ly106G^{+} CD11b^{+} neutrophil recruitment to the lungs of *Cybb*$^{-/-}$ mice 50 days following infection (gated on live/singlets/CD45^{+}). **J.** Quantification of the absolute number of neutrophils recruited to the lungs 1150 days following high dose infection for wild type and *Cybb*$^{-/-}$ mice is shown (mean $^{+/-}$ s.d). ** p-value <.01 by one-way ANOVA with tukey correction. Representative of two experiments with 5 mice per group. **K.** Lung homogenates from uninfected *Cybb*$^{-/-}$ mice and wild type or *Cybb*$^{-/-}$ mice infected for 1250 days following high dose aerosol were probed for IL-1β by ELISA (mean $^{+/-}$ s.d). ** p-value <.01 by unpaired two-tailed t-test. Results shown in G-J are representative of 2 independent experiments with 5 mice per group. ** p-value <.01 by unpaired two-tailed t-test.

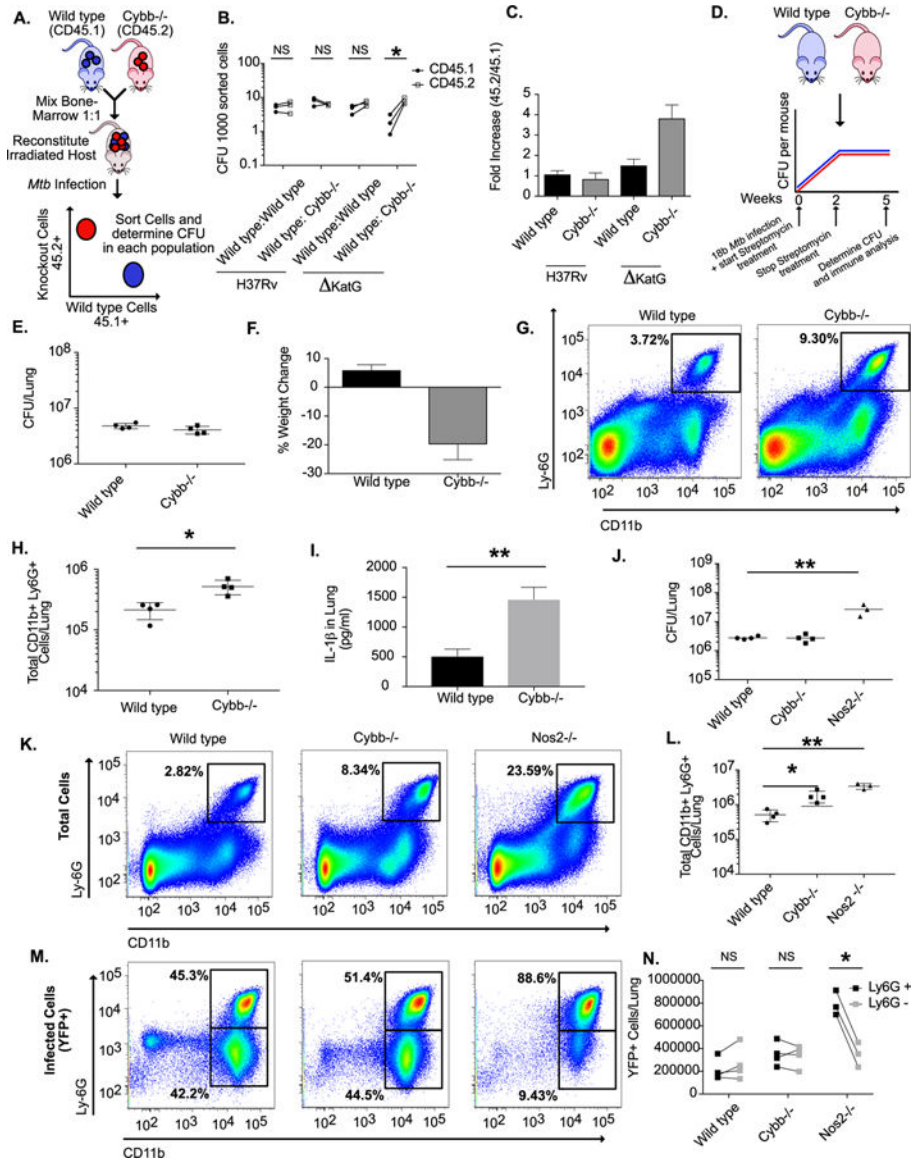

Figure 2. The primary protective role of Cybb is anti-inflammatory.

A. Schematic for the generation of mixed bone marrow chimeras. Mixed bone marrow chimeras were infected by low dose aerosol with either H37Rv or ΔKatG mutant. Five weeks following infection CFU levels were determined in purified hematopoietic cells of indicated genotypes. **B.** Shown are the normalized CFU per sorted cells in each population from each mouse. * p<.05 by unpaired two-tailed t-test. **C.** The fold-increase of bacterial levels in $CD45.2^{+}$ cells (experimental) compared to $CD45.1^{+}$ cells (wild type control) (mean $^{+/-}$ s.d.). The results in B and C are representative of three independent experiments with 3–4 mice per group. **D.** Schematic for streptomycin-dependent infection. Wild type and *Cybb* $^{-/-}$ mice were infected intratracheally with *Mtb* strain 18b and treated for two weeks daily with streptomycin. Mice were then removed from streptomycin for three weeks halting active growth of the bacteria. **E.** Five weeks after infection the total levels of viable *Mtb* in the lungs was determined by CFU plating on streptomycin (mean $^{+/-}$ s.d.). **F.** Percentage

weight loss (mean change $^{+/-}$ s.d) from Day 0 to Day 35 was determined for wild type and *Cybb*$^{-/-}$ mice. **G.** Representative flow cytometry plot showing increased Ly6G^{+} CD11b^{+} neutrophil recruitment to the lungs of *Cybb*$^{-/-}$ mice 5 weeks following infection (gated on live/singlets/CD45^{+}). **H.** Quantification of neutrophil recruitment to the lungs at the indicated time points following infection for wild type and *Cybb*$^{-/-}$ mice is shown as absolute number of Ly6G^{+} CD11b^{+} cells per lung (mean $^{+/-}$ s.d). * p-value <.05 by unpaired two-tailed t-test. Data in E-H are representative of 4 independent experiments with 4–5 mice per group. **I.** Lung homogenates from wild type or *Cybb*$^{-/-}$ mice infected with 18b were probed for IL-1β by ELISA (mean $^{+/-}$ s.d). ** p-value <.01 by unpaired two-tailed t-test. **J.** Following low dose aerosol infection with sfYFP H37Rv (Day 0 of ~50–100 colony forming units, cfu) total bacterial burden (expressed in cfu, mean $^{+/-}$ s.d.) was determined in the lungs of wild type, *Cybb*$^{-/-}$ or Nos2$^{-/-}$ mice 4 weeks post-infection. ** p-value <.01 by one-way ANOVA with tukey correction. **K.** Shown are representative flow cytometry plots from each genotype of total Ly6G^{+} CD11b^{+} cells in the infected lungs. **L.** Quantification of total neutrophil recruitment to the lungs of the indicated genotypes four weeks following infection (mean $^{+/-}$ s.d.). ** p-value <.01 * p-value <.05 by one-way ANOVA with tukey correction. **M.** Shown are representative flow cytometry plots from each genotype of infected (YFP^{+} Ly6G^{+} CD11b^{+}) cells in the lung. **N.** Enumeration of infected (YFP^{+}) neutrophils (Ly6G^{+} CD11b^{+}) or monocytes/macrophages (Ly6G- CD11b^{+}) in the indicated genotypes. * p-value <.05 by unpaired two-tailed t-test. Data in J-N are representative of three independent experiments with 3–5 mice per group.

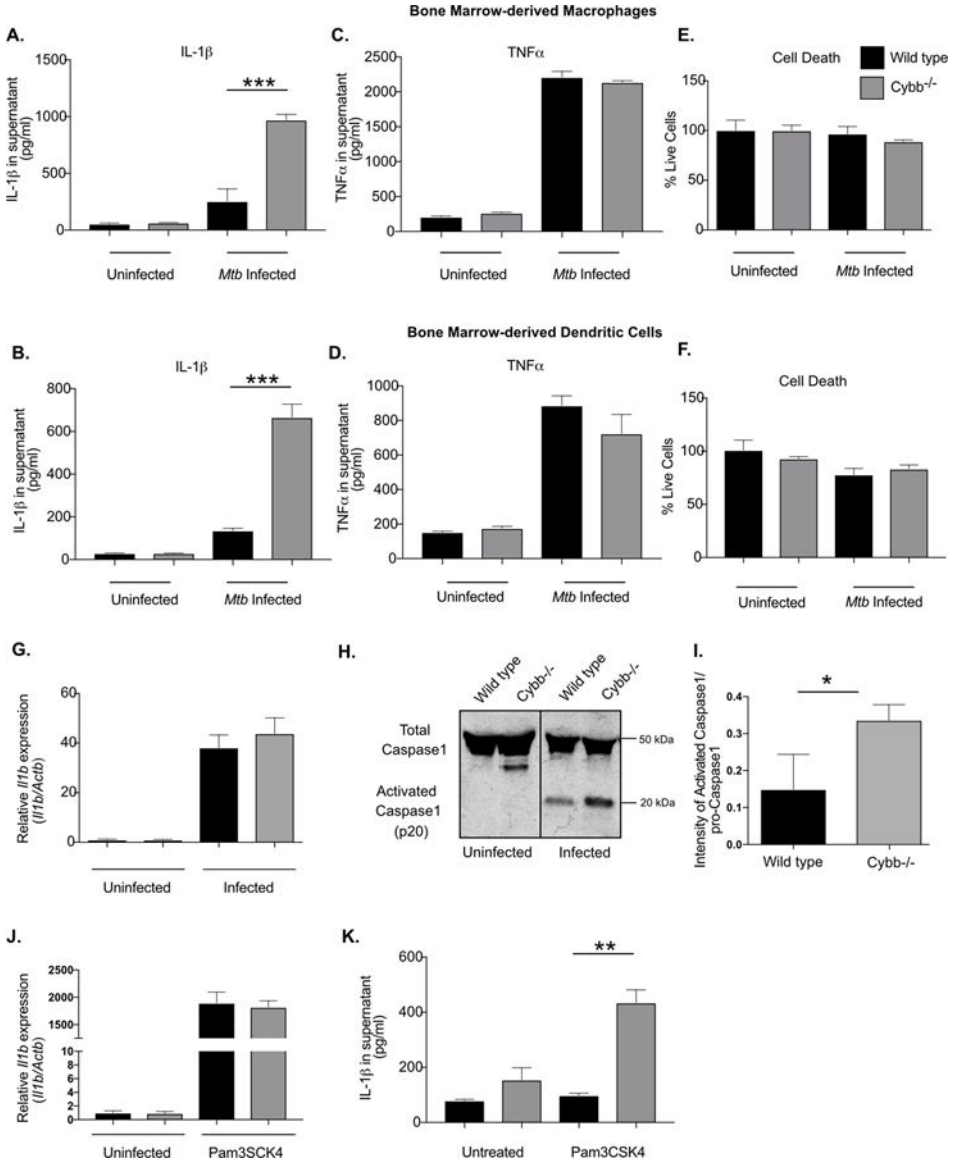

Figure 3. Cybb controls Caspase1 activation in macrophages and dendritic cells during *Mtb* infection.

Bone marrow-derived macrophages (BMDMs) or Bone marrow-derived dendritic cells (BMDCs) from wild type or *Cybb*$^{-/-}$ mice were left untreated or infected with *Mtb* for 4 hours then washed with fresh media. 18 hours later supernatants were harvested and the levels of **A.** and **B.** IL-1β and **C.** and **D.** TNFα were quantified in the supernatants by ELISA. Shown is the mean of 4 biological replicates normalized to a standard curve $^{+/-}$ s.d. *** p<.001 by unpaired two-tailed t-test. **E.** and **F.** Viability of remaining cells was determined by quantifying ATP via luminescence and compared to cells at 4 hours post-infection (mean % viability $^{+/-}$ s.d.). Data in A, C and E are representative of five independent experiments with at least 3 biological replicates per experiment. Data in B, D and F are representative of three independent experiments with 4 biological replicates per experiment. **G.** Relative RNA expression of *Il1b* (compared to β-Actin) was determined from wild type and *Cybb*$^{-/-}$ BMDMs left untreated or infected for 24 hours with *Mtb* (mean

$^{+/-}$ s.d.) by qRT-PCR. Data are representative of two independent experiments with 3–4 biological replicates per group. **H.** Immunoblot analysis was used to assess the activation of Caspase 1 from Wild type and *Cybb*$^{-/-}$ BMDMs infected for 24 hours with *Mtb*. Data are representative of 3 independent experiments with at least 3 biological replicates analyzed per experiment. **I.** Immunoblots were quantified by comparing the intensity of activated p20-Caspase 1 to total pro-Caspase1 bands. Quantification was done on three biological replicates. * $p<.05$ by unpaired two-tailed t-test. **J.** Relative RNA expression of *Il1b* (compared to *Actb*) was determined from wild type and *Cybb*$^{-/-}$ BMDMs left untreated or treated with Pam3CSK4 for 24 hours (mean $^{+/-}$ s.d.) by qRT-PCR. Data are representative of two independent experiments with 3–4 biological replicates per group. **K.** Wild type and *Cybb*$^{-/-}$ BMDMs were left untreated or treated with PAM3CSK4 for 12 hours, supernatants were harvested and the levels of IL-1β were quantified by ELISA (mean $^{+/-}$ s.d.). ** $p<.01$ by unpaired two-tailed t-test. Data are representative of three independent experiments with 4 biological replicates per experiment.

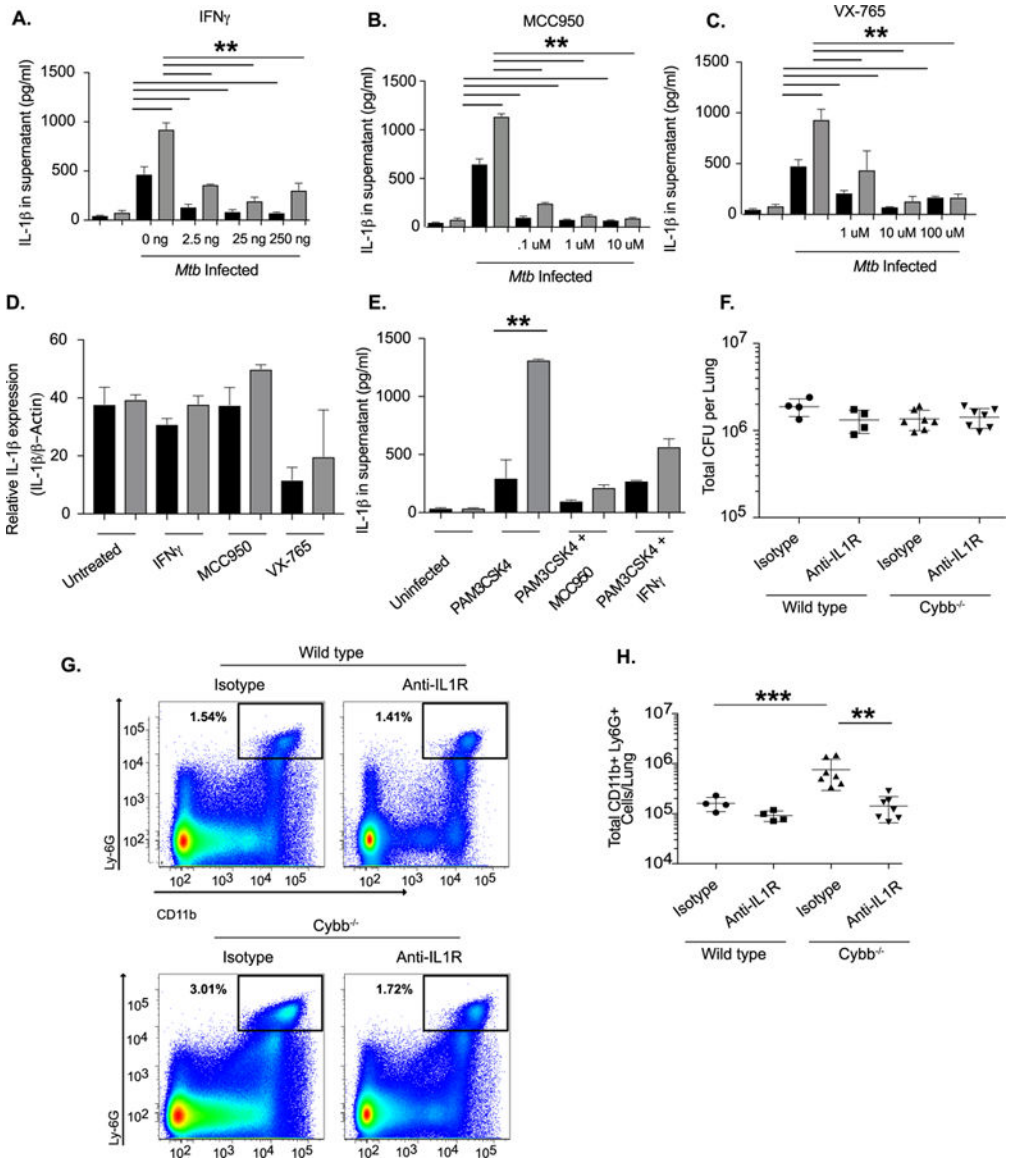

Figure 4. Hyper-inflammation in *Cybb*$^{-/-}$ is reversed by inflammasome and IL1 inhibition.

A. Wild type (Black Bars) and *Cybb*$^{-/-}$ (Grey Bars) BMDMs were left untreated or treated with the indicated concentrations of IFNγ for 12 hours. Cells were then infected with *Mtb* for 4 hours then washed with fresh media. 18 hours later supernatants were harvested and levels of IL-1β from each condition were quantified by ELISA (mean $^{+/-}$ s.d.). ** p-value <.01 * p-value <.05 by one-way ANOVA with tukey correction. Data are representative of three independent experiments with at least 3 biological replicates per experiment. **B.** Wild type and *Cybb*$^{-/-}$ BMDMs were left untreated or treated with the indicated concentrations of MCC950 for 2 hours. Cells were then infected with *Mtb* for 4 hours then washed with fresh media with inhibitor. 18 hours later supernatants were harvested and levels of IL-1β from each condition were quantified by ELISA (mean $^{+/-}$ s.d.). ** p-value <.01 by one-way ANOVA with tukey correction. Data are representative of three independent experiments with at least 3 biological replicates per experiment. **C.** Wild type and *Cybb*$^{-/-}$ BMDMs were

left untreated or treated with the indicated concentrations of VX-765 for 2 hours. Cells were then infected with *Mtb* for 4 hours then washed with fresh media with inhibitor. 18 hours later supernatants were harvested and levels of IL-1β from each condition were quantified by ELISA (mean $^{+/-}$ s.d.). ** p-value <.01 by one-way ANOVA with tukey correction. Data are representative of three independent experiments with at least 3 biological replicates per experiment. **D.** Relative RNA expression of IL-1β (compared to b-Actin) was determined from wild type and *Cybb*$^{-/-}$ BMDMs left infected for 24 hours with *Mtb* in the presence or absence of the indicated inhibitors (mean $^{+/-}$ s.d.) by qRT-PCR. Data are representative of two experiments with 4 biological replicates per group. **E.** Wild type and *Cybb*$^{-/-}$ BMDMs were left untreated or treated 25ng/ml IFNγ or 1μM MCC950 overnight. The following day cells were treated with PAM3CSK4 for 12 hours, supernatants were harvested and the levels of IL-1β were quantified by ELISA (mean $^{+/-}$ s.d.). ** p<.01 by unpaired two-tailed t-test. Data are representative of two independent experiments with 4 biological replicates per experiment. **F.** Wild type and *Cybb*$^{-/-}$ mice were infected intratracheally with *Mtb* strain 18b and treated for two weeks daily with streptomycin then were injected every other day for two weeks with 200ug of either isotype control antibody or anti-IL1R antibody. The total levels of viable *Mtb* in the lungs was determined by CFU plating on streptomycin (mean $^{+/-}$ s.d.) with 4–7 mice per group. **G.** Representative flow cytometry plot showing Ly6G^{+} CD11b^{+} neutrophil recruitment to the lungs of *Cybb*$^{-/-}$ mice during control and IL1R blockade conditions (gated on live/singlets/CD45^{+}). **H.** Quantification of neutrophil recruitment to the lungs at the indicated time points following infection for wild type and *Cybb*$^{-/-}$ mice during control and IL1R blockade conditions is shown as an absolute number of Ly6G^{+} CD11b^{+} cells per lung (mean $^{+/-}$ s.d). *** p-value <.001 ** p-value <.01 by one-way ANOVA with tukey correction. Data in F-G are representative of two independent experiments with 4–7 mice per group.